C9orf72 functions in the nucleus to regulate DNA damage repair

Liying He, Jiaqi Liang, Chaonan Chen, Jijun Chen, Yihui Shen, Shuangshuang Sun, and Lei Li

Supplementary Figures S1-S7 and legends

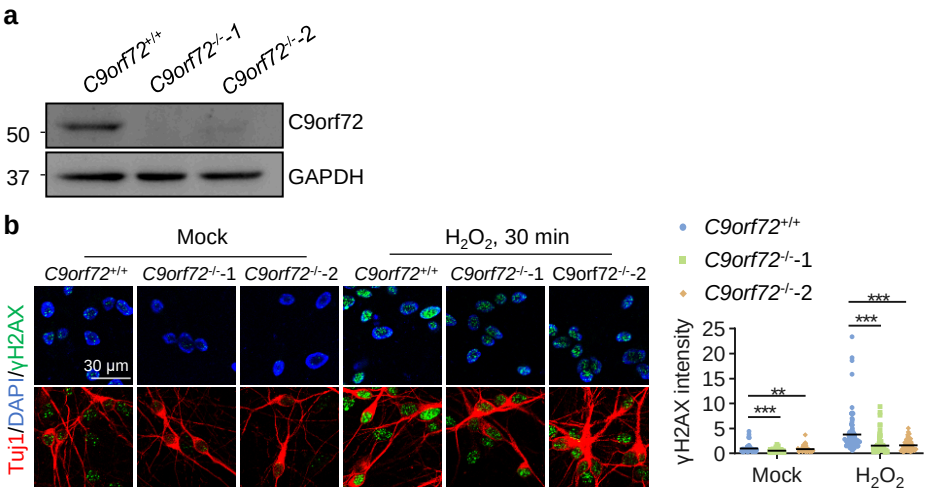

Fig. S1. Attenuated phosphorylation of H2AX in induced neurons.

(**a**) Generation of *C9orf72* KO induced pluripotent stem cells (iPSC) lines by CRISPR-Cas9. *C9orf72* KO cell lines were validated by Immunoblot.

(**b**) Decreased phosphorylation of H2AX in C9orf72-dificient induced neurons. WT and *C9*KO induced neurons were treated with or without H_2O_2 (200 μM) for 30 min, followed by fixation and staining with anti-γH2AX (green) and anti-Tuj1 (red) antibodies. Quantitative analysis of γH2AX intensity. Data are mean (n = 55-100 cells from 3 independent experiments; one-way ANOVA; **, $p < 0.01$; ***, $p < 0.001$).

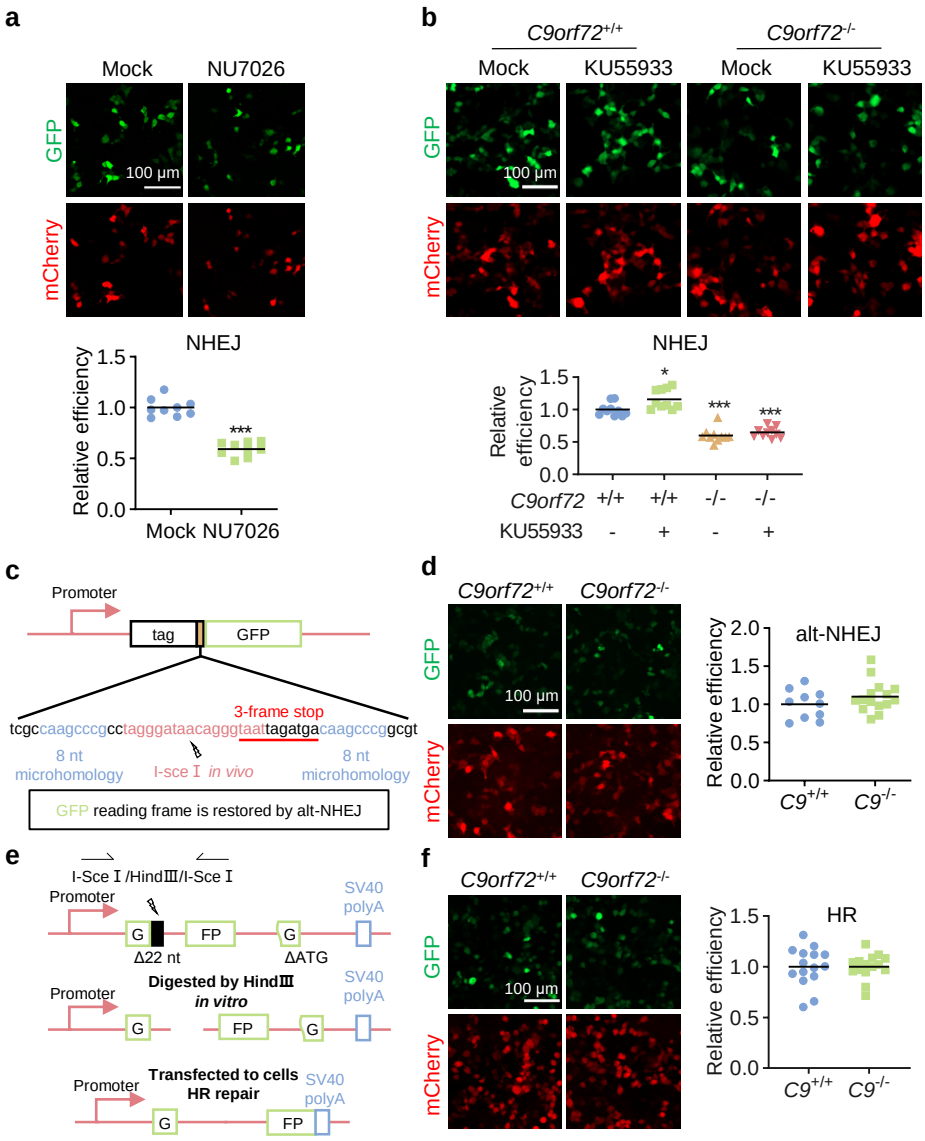

Fig. S2. DNA damage repair assays in C9orf72-deficient cells.

(**a**) Impaired NHEJ repair in HEK293T cells treated with DNA-PKcs inhibitor NU7026. HEK293T cells were transfected with cleaved NHEJ reporter and mCherry constructs. The transfected cells were treated with NU7026, and the GFP-positive cells were counted as successful NHEJ. Data are mean (n = 9 images from 3 independent experiments; unpaired t test; ***, $p < 0.001$).

(**b**) NHEJ repair efficiency in C9orf72-deficient cells treated with ATM inhibitor KU55933. HEK293T cells with indicated genotypes were transfected with cleaved NHEJ reporter and mCherry constructs. The transfected cells were treated with KU55933 and the GFP-positive cells were counted as successful NHEJ. Data are mean (n = 10 images from 3 independent experiments; Two-way ANOVA; *, $p < 0.05$; ***, $p < 0.001$).

(**c-d**) Similar alt-NHEJ repair efficiency in WT and *C9orf72* KO cells. (**c**) Diagram of alt-NHEJ reporter construct. (**d**) HEK293T cells were transfected with alt-NHEJ reporter, I-SceI, and mCherry constructs. The GFP-positive cells were counted as successful alt-NHEJ. Data are mean (n = 10-15 images from 3 independent experiments; unpaired t test).

(**e-f**) Similar HR repair efficiency in WT and *C9orf72* KO cells. (**e**) Diagram of HR reporter construct. (**f**) HEK293T cells were transfected with cleaved HR reporter and mCherry constructs. The GFP-positive cells were counted as successful HR. Data are mean (n = 15 images from 3 independent experiments; unpaired t test).

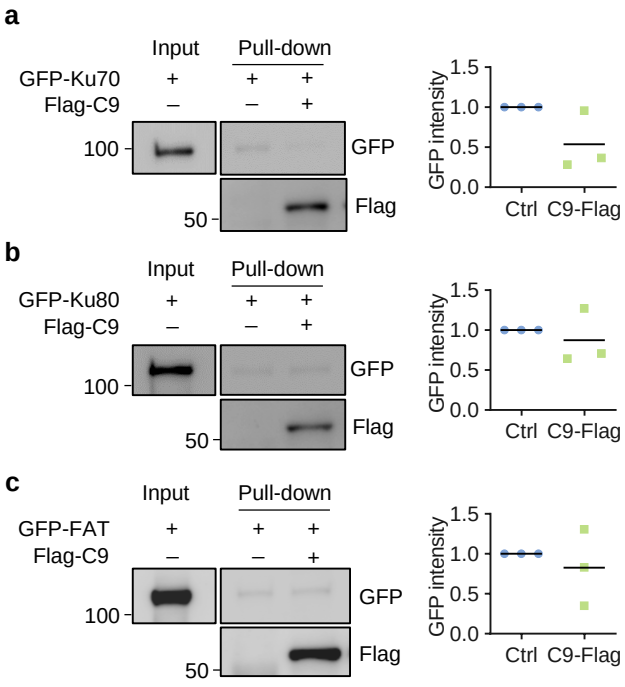

Fig. S3. C9orf72 did not interact with Ku70, Ku80 or FAT domain of DNA-PKcs.

(**a-c**) C9orf72 did not interact with Ku70 or Ku80 in *in vitro* pull-down assay. Flag-C9orf72 was purified from HEK293T cells and incubated with purified GFP-Ku70 (**a**), GFP-Ku80 (**b**), or GFP-FAT (**c**), respectively. None of the proteins interacted with C9orf72 in the pull-down assay. Quantitative analysis of GFP intensity. Data are mean (n = 3 independent experiments).

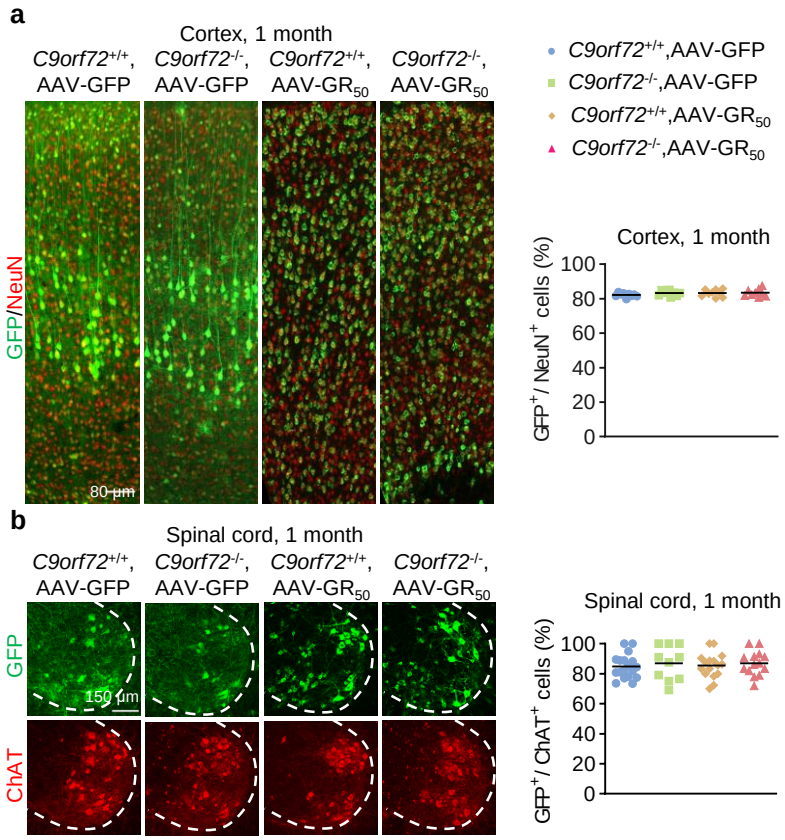

Fig. S4. High efficiency of AAV infection in the motor cortex and spinal cord.

(**a**) AAV infection efficiency in motor cortex at 1 month of age. The AAV9 expressing either GFP or GFP-poly-GR50 was injected into cerebroventricular region at postnatal day 0 (P0). The percentage of GFP-positive cells was counted at 1 month of age. Data are mean (n = 9 sections of 3 mice; one-way ANOVA).

(**b**) AAV infection efficiency in the spinal cord at 1 month of age. The AAV9 expressing either GFP or GFP-poly-GR50 was injected into cerebroventricular region at postnatal day 0 (P0). The spinal cord slices were stained with anti-ChAT antibody to label motor neurons. The percentage of GFP-positive motor neurons was counted at 1 month of age. Data are mean (n = 10-18 sections of 3 mice; one-way ANOVA).

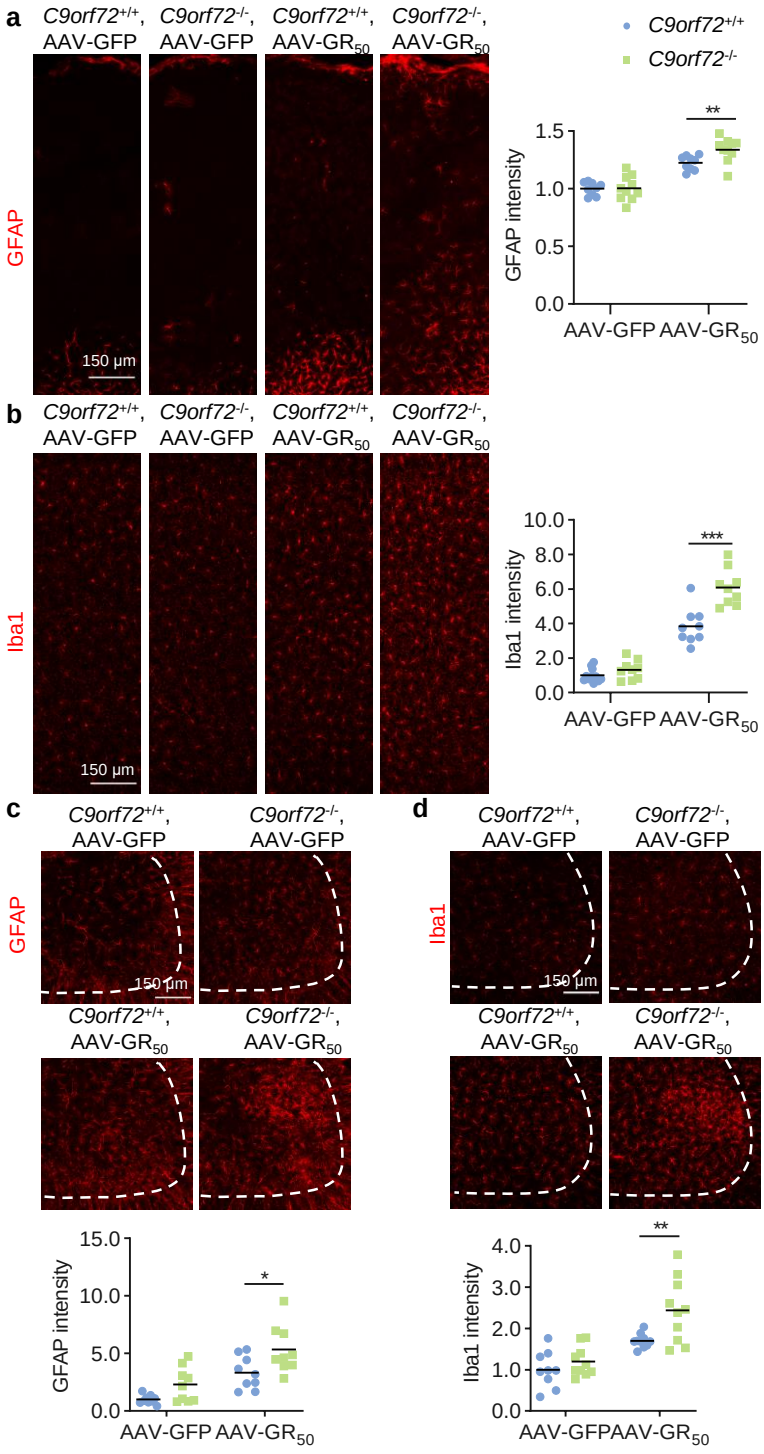
a
C9orf72+/+, AAV-GFP
C9orf72-/-, AAV-GFP
C9orf72+/+, AAV-GR50
C9orf72-/-, AAV-GR50
GFAP
150 µm
C9orf72+/+
C9orf72-/-
GFAP intensity
**
AAV-GFP
AAV-GR50
b
Iba1
***
Iba1 intensity
c
d
*
**

Fig. S5. Increased activation of astrocytes and microglia in the cortex and spinal cord of *C9orf72*$^{-/-}$, AAV-GR$_{50}$ mice.

(**a-b**) Increased reactive astrocytes and microglia in the motor cortex of *C9orf72*$^{-/-}$, AAV-GR$_{50}$ mice at 6 months of age. Brain slices of indicated genotypes were stained with anti-GFAP antibody to label reactive astrocytes (**a**), and anti-Iba1 antibody to label reactive microglia (**b**) in the motor cortex. Quantitative analysis of intensities of reactive astrocytes (**a**) and microglia (**b**) (n = 9-11 sections of 3 mice).

(**c-d**) Increased reactive astrocytes and microglia in the spinal cord of *C9orf72*$^{-/-}$, AAV-GR$_{50}$ mice at 6 months of age. Spinal cord slices of indicated genotypes were stained with anti-GFAP antibodies to label reactive astrocytes (**c**), and anti-Iba1 to label reactive microglia (**d**) in the spinal cord. Quantitative analysis of intensities of reactive astrocytes (**c**) and microglia (**d**) (n = 9-10 sections of 3 mice). Data are mean (unpaired t test; *, $p < 0.05$; **, $p < 0.01$; ***, $p < 0.001$).

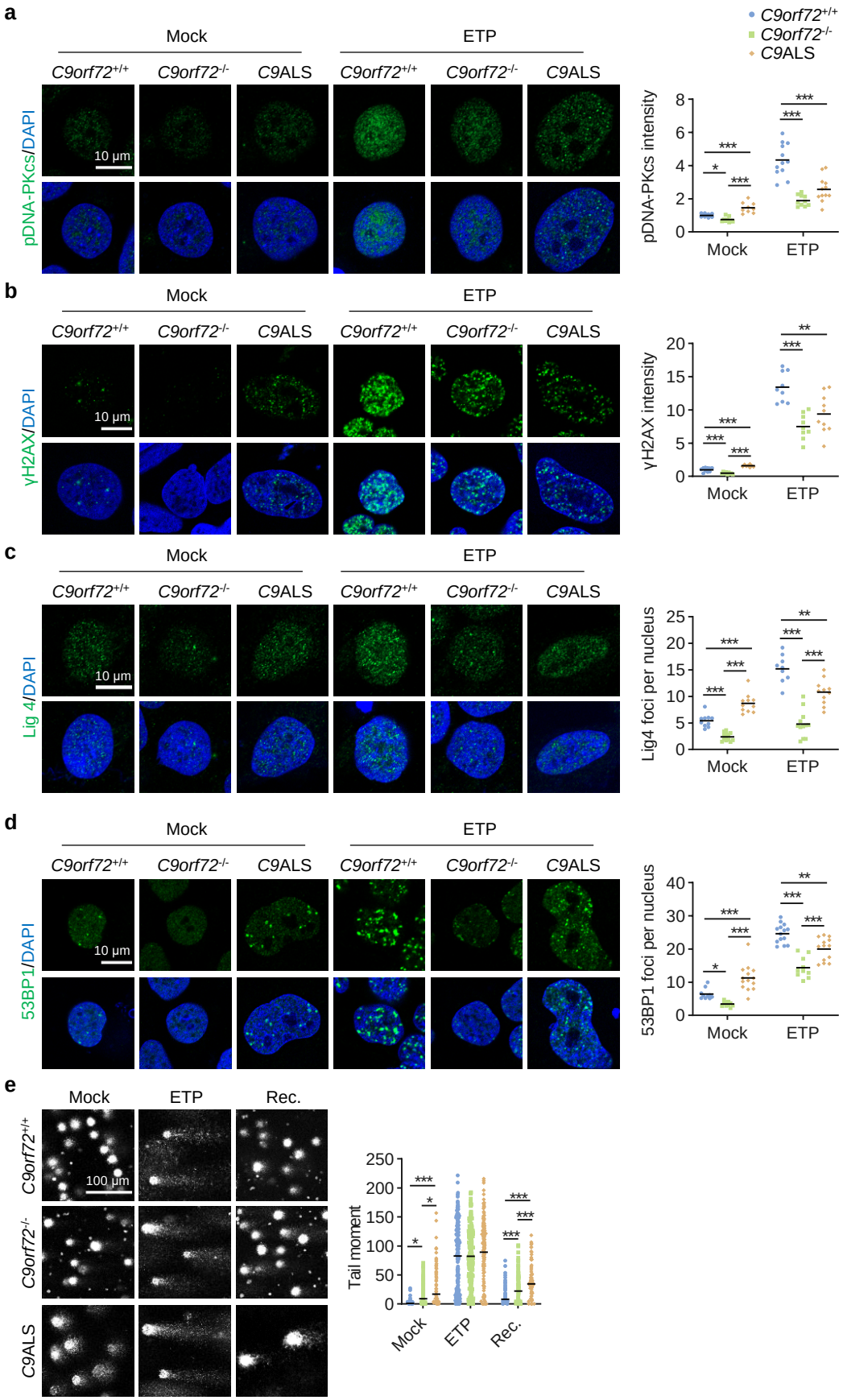
a
Mock
ETP
C9orf72+/+
C9orf72-/-
C9ALS
pDNA-PKcs/DAPI
10 μm
pDNA-PKcs intensity
b
γH2AX/DAPI
γH2AX intensity
c
Lig 4/DAPI
Lig4 foci per nucleus
d
53BP1/DAPI
53BP1 foci per nucleus
e
Rec.
100 μm
Tail moment

Fig. S6. Impaired NHEJ repair in neural progenitor cells derived from *C9*ALS patient.

(**a-d**) Neural progenitor cells derived from healthy control or *C9*ALS patient were treated with 10 μM ETP for 30 min, followed by fixation and staining with anti-pDNA-PKcs (**a**), anti-γH2AX (**b**), anti-Lig4 (**c**) and anti-53BP1 (**d**) to reveal NHEJ repair signal transduction. Quantitative analysis of pDNA-PKcs (**a**) and γH2AX (**b**) intensities and foci number of Lig4 (**c**) and 53BP1 (**d**). Data are mean (n = 9-14 images of 3 independent experiments; One-way ANOVA; *, $p < 0.05$; **, $p < 0.01$; ***, $p < 0.001$).

(**e**) Impaired DNA damage repair in *C9*ALS patient-derived neural progenitor cells. Cells with indicated genotypes were treated with 10 μM ETP for 2 h (ETP). After withdrawal of ETP, neural progenitor cells were allowed to recover for 24 h to repair DNA damage (Rec.). DNA damage was assessed by a comet assay. Quantitative analysis of tail moment. Data are mean (n = 162-256 cells from 3 independent experiments; Two-way ANOVA; *, $p < 0.05$; ***, $p < 0.001$).

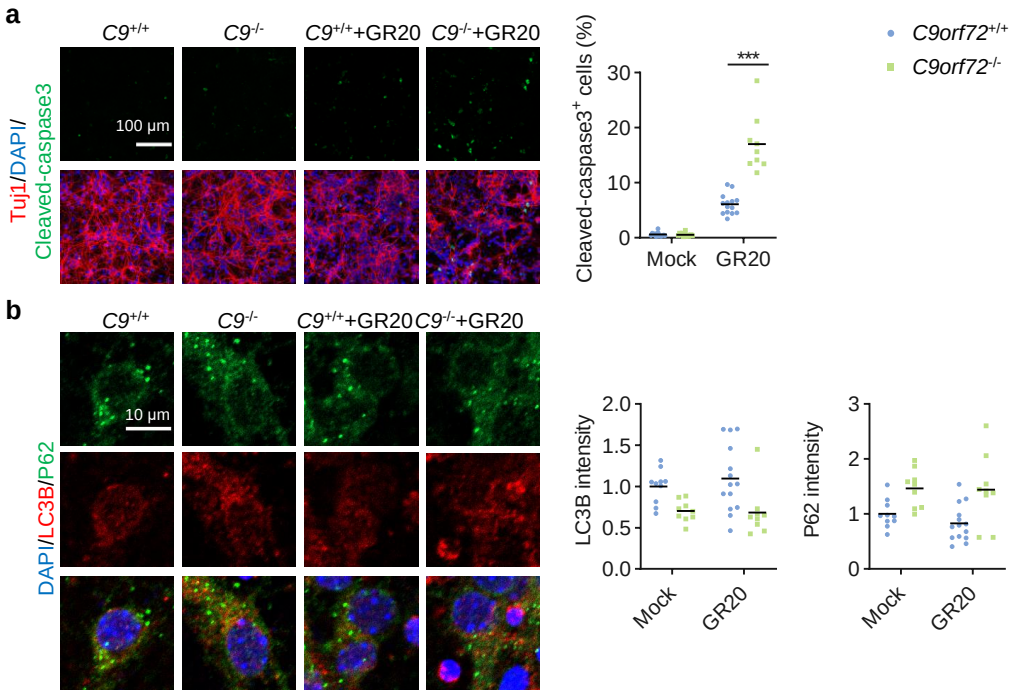

Fig. S7. Increased apoptosis in the poly-GR-treated *C9orf72*$^{-/-}$ neurons.

(**a-b**) The cortical neurons with indicated genotypes were cultured for 48 h and treated with poly-GR peptide (10 μM) for 48 h. The neurons were fixed and stained with anti-Cleaved caspase 3 (**a**) to analyze apoptosis, or anti-LC3B and anti-P62 (**b**) to analyze autophagy. Quantitative analysis of Cleaved-caspase 3 intensity (**a**); LC3B and P62 intensities (**b**). Data are mean (n = 9-14 images of 3 independent experiments; Two-way ANOVA; ***, $p < 0.001$).